Available online at www.sciencedirect.com
SCIENCE DIRECT®
Catalysis Today 98 (2004) 393–402
CATALYSIS TODAY
www.elsevier.com/locate/cattod

Mechanistic and kinetic studies of NO_x storage and reduction on $Pt/BaO/Al_2O_3$

Rachel L. Muncrief, Pranav Khanna, Karen S. Kabin, Michael P. Harold*

Department of Chemical Engineering, University of Houston, 4800 Calhoun Road, S222 Engineering Bldg. 1, Houston, TX 77204-4004, USA

Available online 29 September 2004

Abstract

NO_x storage and NO oxidation experiments have been carried out on a model $Pt/BaO/Al_2O_3$ catalyst powder in order to elucidate kinetic and thermodynamic limitations. Uptake of NO on a pre-oxidized catalyst reveals the existence of multiple regimes. The short-term storage is a sensitive function of storage time, but is nearly independent of temperature whereas the long-time storage has much slower kinetics and is a non-monotonic function of temperature. A simple steady-state reactor model is developed that predicts NO oxidation conversion and the limiting NO_x storage. The model predicts that full barium utilization is thermodynamically feasible even under kinetically limiting conditions of incomplete NO oxidation. However, apparent NO_x diffusion limitations prevent complete utilization. Storage and reduction (with propylene) experiments indicate that less than 10% of the barium is needed to achieve high NO_x conversion (>85%) at moderate space velocity. At higher temperature both NO oxidation and barium nitrate formation are thermodynamically limited, both of which adversely impact the NO_x reduction. Thermogravimetric measurements corroborate a physical picture in which only a small fraction of barium is utilized during lean/rich cycling protocols giving high NO_x conversion.

Keywords: NO_x; Diesel; Lean-burn; Emissions; NO_x trap; NO_x storage and reduction

1. Introduction

Diesel and lean-burn gasoline engines operate with oxygen in excess of stoichiometric requirements for combustion. This leads to increased fuel efficiency but it also complicates the reduction of nitrogen oxides (NO_x). NO_x reduction is straightforward in a net reducing atmosphere over precious metal catalysts, but this condition does not exist in the exhaust of lean-burn engines.

One promising technology that is being studied to combat this problem is NO_x storage and reduction (NSR) or the so-called ''NO_x trap'' which was first proposed by Toyota in the mid-1990s for lean-burn gasoline engines [1]. NSR involves the use of a bi-functional precious metal catalyst containing a NO_x storage component, typically an alkali earth oxide compound such as barium oxide. The basic steps of NSR are as follows: while the engine is running lean, NO and oxygen combine on platinum to form NO_2, which is subsequently trapped on the storage component in the form of a nitrite or nitrate. The next step is to introduce a reductant into the system, either by temporarily running the engine rich or by directly injecting fuel or reformed fuel (CO, H_2 mixture) into the exhaust stream. The reductant has two functions. The first function is to react with the barium nitrites and nitrates, thereby returning the barium to its initial form and either releasing NO/NO_2 or reducing NO_x to nitrogen. The second function is to react with oxygen present in the exhaust in order to create a temporary fuel rich environment, freeing up sites on the Pt for NO_x reduction to occur. In the fuel rich environment NO_x is converted to nitrogen on Pt sites made vacant by the reaction between surface oxygen and hydrocarbon – as in conventional three-way catalytic converters. The extent to which NO_x reduction occurs by nitrite/nitrate decomposition or selective catalytic reduction is a complex function of the operating conditions and catalyst composition.

Many studies have reported the beneficial effects of lean/rich cycling over standard steady-state conversion. Researchers at Toyota were the first to show high (>90%)

* Corresponding author. Tel.: +1 713 743 4304; fax: +1 713 743 4323.
E-mail address: mharold@uh.edu (M.P. Harold).

0920-5861/$ – see front matter © 2004 Elsevier B.V. All rights reserved.
doi:10.1016/j.cattod.2004.08.004

conversion efficiency for an optimized catalyst and control system during lean/rich cycling using a NO_x trap catalyst [2]. Muncrief et al. [3] reported that cyclic operation can significantly increase the conversion from its steady-state level. For example, a 10 s fuel rich pulse resulted in a time-averaged conversion exceeding 90%, while a continuous feed having the same composition as the cycle averaged feed resulted in a conversion of only 20%. Jirat et al. in a modeling study reported that the steady-state conversion of 40% can be increased to over 90% with cycling [4].

Although NSR catalysts are emerging as a commercially viable approach for lean NO_x reduction, certain mechanistic and kinetic issues are not fully understood. A number of studies have appeared during the last few years that have focused on the storage of NO_x on the alkali earth metal during the lean phase of the cycle. Aspects of the storage that have been studied include the role of the support, the storage component, and the precious metal [5–7], the state of the barium during NO_x storage [8–11], the capacity of the barium for NO_x storage [12–14], the proximity of NO_x storage sites to platinum sites [15,16], the effect of other feed components (such as water and CO_2) [17–19], the effect of catalyst temperature [16,20–22], and the effect of the concentrations of NO, NO_2 and O_2 [2,4,23]. Issues of particular pertinence to the current study are highlighted next.

Many groups in the literature have reported maximum NO_x storage occurring between 300 and 400 °C on Pt/BaO/Al_2O_3 catalysts in a feed containing NO and O_2. For example, Lietti et al. [22] found the maximum storage occurring at 300 °C, Mahzoul et al. [15] found maximum NO_x storage at 350 °C, Fridell et al. [24] observed a maximum in NO_x storage at 380 °C, and Li et al. [10] found maximum NO_x storage at 400 °C. Many variables have been reported in the literature that affect the NO_x storage capacity (or barium utilization) on Pt/BaO/Al_2O_3 catalyst. Forzatti and co-workers [14,22] found that the amount of NO_x species adsorbed was greater when NO_2 was used in the feed as opposed to NO/O_2. In addition they found that approximately 20% of the barium is involved in the storage when NO/O_2 feeds are used as opposed to 50–60% when NO_2 feeds are used. On the other hand, Fridell et al. [24] reported that the storage of NO_x is similar whether NO/O_2 or NO_2 are in the feed gas. Li et al. [10] reported that NO_x storage capacity is higher for a pre-reduced catalyst than a pre-oxidized catalyst. Finally, Mahzoul et al. [15] also found that adsorption capacity depends on experimental conditions; for example, increasing concentrations of NO_2 or O_2 in the feed will increase the NO_x storage capacity.

The mechanism of NO_x storage is another contested topic with many different proposals appearing in the literature. Forzatti and co-workers [14,22,23,25] have found using in situ FTIR that NO is stored according to two different mechanisms (both promoted by platinum); the first occurs through the formation of surface nitrites that convert to nitrates; the second occurs via the oxidation of NO to NO_2 on the Pt, followed by NO_2 migration to the Ba phase and subsequent nitrate formation. However, when NO_2 is the NO_x species, the first mechanism does not occur while the second mechanism does not require platinum to proceed. In a series of papers, Fridell and co-workers [13,16,24,26,27] employed a combination of storage measurements, storage and reduction experiments, and micro-kinetic modeling. They found that the NO_x storage capacity was thermodynamically limited at temperatures above 350 °C but below this temperature the conversion of NO to NO_2 was kinetically limited. They were able to fit a kinetic model to the NO oxidation at low temperatures, and determined that the formation of NO_2 is a crucial step for NO_x storage. Their proposed mechanism of NO_x storage proceeds by NO_2 chemisorption at barium sites to form nitrites and nitrates followed by a surface redox step to form nitrate–nitrite pairs. Oxidation of the remaining nitrite forms an all-nitrate final product. They concluded that platinum promotes NO_x desorption which is attributed to a spillover of NO_x from the storage sites to platinum. Li et al. [10] and Mahzoul et al. [15] propose similar mechanisms, in which two kinds of Pt sites operate during the NO_x storage; the first site type is responsible for NO chemisorption and the second for oxidizing the NO. Huang et al. [5] found that nitrite and NO_2 adspecies were the intermediates formed during the formation of the nitrate. Schmitz and Baird [12] studied the adsorption of NO and NO_2 on barium oxide. They found using XPS that NO will primarily form nitrites and NO_2 nitrates. For the Pt/BaO system they suggest that NO_2 formed by NO oxidation on the Pt can either dissociatively adsorb to form a nitrite or combine with surface nitrites to form nitrates.

Certain key aspects concerning the mechanistic and kinetic features of NO_x storage have yet to be clarified, such as the dependence of NO_x storage kinetics on storage time and temperature, and how these factors impact barium utilization and NO_x conversion during NO_x storage and reduction. The present study provides new insight about NO_x storage on Pt/BaO/Al_2O_3 catalysts through a combination of NO_x storage kinetics, TGA measurements during NO_x storage and reduction, and modeling. We examine the dependence of the storage kinetics on uptake time and temperature, and relate these findings to barium utilization and NO_x storage and reduction performance. A simple model of NO_x storage is used to elucidate the role of NO oxidation and to identify rate controlling processes.

2. Experimental

The model NO_x storage catalyst (powder), Pt/BaO/Al_2O_3 (1/20/100, w/w/w) was prepared using standard impregnation techniques described in detail previously [3]. Elemental platinum concentration was 0.5 ± 0.05 wt.% as measured by ICP-OES (Galbraith Laboratories, Tenn.); elemental barium was 12.32 ± 0.05 wt.%. The deviation between the

Table 1
Composition of the feed gas in the storage and cycling experiments

	Lean (cycling)	Rich (cycling)	Storage only
O_2 (%)	5	5	5
NO (ppm)	500	500	500
C_3H_6 (%)	0.1	2	0

intended and ICP-measured loadings suggests some solution loss during the impregnation. The catalyst had a surface area of 140 m^2/g, an average particle size of 55 μm, and a platinum dispersion of 47%. The platinum dispersion was measured by hydrogen-pulse chemisorption. The catalyst surface area was measured with BET (Beckman Coulter, model SA3100) using N_2 adsorption.

A comprehensive study of NO_x storage and reduction was carried out with the said catalyst powder in a flow-through reactor setup [3]. In the current study the feed gas contained a mixture of NO, C_3H_6, and O_2 in a nitrogen carrier; actual concentrations used are shown in Table 1. Oxygen was fixed at 5% during the rich period to simulate hydrocarbon injection into a diesel exhaust of fixed composition. The flow rates of the gases were controlled with precision mass flow controllers (MKS), programmed using LabTech® software. The gases were mixed in an in-line static mixer, and fed to a catalytic reactor (described in more detail below).

Pulsing of reductant was achieved through computer control of the propylene feed. The reactor effluent gases flowed through heated lines (110 °C) to a gas phase FTIR spectrometer, where the transient species concentrations were then quantified, including NO, NO_2, CO_2, H_2O, CO, C_3H_6 and N_2O. Runs without catalyst indicated some conversion of NO to NO_2 (<2% at 100 °C). We routinely reviewed the product spectra for IR bands of other species during the experiments, such as NH_3. N_2 production was determined as the difference between the total NO_x reacted and NO_x converted to N_2O according to: NO_x to N_2 = NO_x reacted − $2N_2O$ formed. The primary reactor that was utilized was a conventional catalytic microreactor, a quartz tube packed with a small amount of powder catalyst. The catalyst bed temperature was measured while maintaining a constant feed temperature. Unless otherwise specified, the total gas flow rate was kept constant at 200 cm^3/min (at 25 °C, 1 atm). The reactor contained 200 mg of catalyst (0.28 cm^3 volume) without dilution. For the stated flow rate the gas space velocity (GHSV) was about 42,000 h^{-1} (standard conditions 25 °C, 1 atm).

Measurement of the storage properties of the catalyst was accomplished by monitoring the NO_x uptake as a function of the feed temperature and the NO partial pressure. In a typical storage experiment we pretreated the catalyst at 550 °C for 1 h in either O_2 or CO_2 (to form either BaO or $BaCO_3$, respectively). We then fed a mixture of NO and O_2 (in N_2) over the catalyst at 200 cm^3/min for a prescribed length of time. Total NO_x uptake was determined by subtracting the moles of NO_x in the effluent (i.e. NO_x breakthrough) from the total NO fed to the system.

A second catalytic reactor used in the experiment was housed in a Simultaneous Differential Scanning Calorimeter and Thermal Gravimetric Analyzer (TGA). The TGA afforded a precise measure of catalyst weight and temperature during various storage and reaction experiments. The TGA has a sensitivity of 1 μg. In the experiments reported here, 20 mg of catalyst was placed in a ceramic pan affixed on a microbalance in a gas stream flowing at 120 cm^3/min. Because the bulk of the gas bypassed the catalyst, the conversion was differential.

3. Results and discussion

We have previously reported that high time-averaged NO_x conversions can be achieved over a wide range of temperatures by optimizing the reductant feed protocol [3]. Specifically, high time-averaged NO_x conversion (>90%) was sustained with a total cycle time of 70 s, a rich pulse of 10 s and a propylene concentration of about 2%. The conversion drops off at low (<200 °C) and high temperatures (>400 °C). Below the ignition temperature of propylene (ca. 200 °C) the excess feed oxygen is not consumed and therefore rich conditions are not achieved for any part of the cycle. Thus, oxygen remains adsorbed on the Pt, which is known to inhibit NO_x adsorption and dissociation. At sufficiently high temperatures the storage capacity of the catalyst is significantly reduced because of barium nitrate decomposition. We return to this issue below.

The adsorptive storage of NO_x on the $Pt/BaO/Al_2O_3$ powder is a critical step in the NSR process. Fig. 1 shows typical NO_x storage data obtained without a co-feed or pulse of propylene. Shown is the concentration of NO fed to the system as well as the NO_x breakthrough versus time. In this experiment we fed a mixture of NO and oxygen over a pre-oxidized catalyst at 350 °C for 1 h. The area between the NO_x breakthrough curve and the dashed line (NO_x feed concentration) represents the NO_x that is trapped by the catalyst. Notice that initially there is no breakthrough (at these conditions no measurable breakthrough occurs until

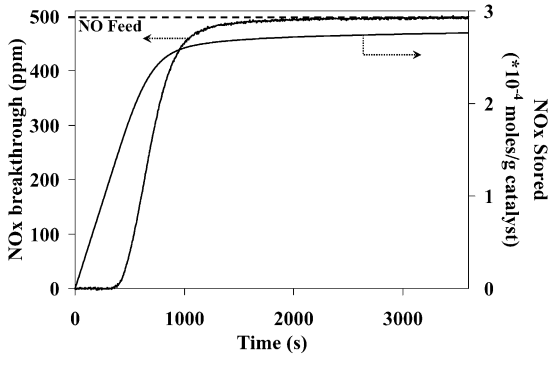

Fig. 1. NO_x breakthrough and cumulative NO_x storage on a $Pt/BaO/Al_2O_3$ catalyst in a feed of 500 ppm NO and 5% O_2 and a feed temperature of 350 °C.

360 s have lapsed). This is followed by a period of slow increase in the effluent NO_x concentration and a very slow approach to the inlet NO_x concentration. These breakthrough data can be cast in terms of total moles of NO_x stored per gram of catalyst. At the conditions of the particular experiment, the NO storage approached 2.8×10^{-4} mol NO/g cat after 1 h of exposure. This corresponds to about 15% of barium utilization, assuming a 2 to 1 N:Ba ratio.

These NO_x breakthrough attributes have been shown in many previous NO_x storage studies. The multi-stage storage process has typically been interpreted with several mechanisms. Li et al. [10,15] proposed that multiple barium sites in the form of $BaAl_2O_3$ and $BaCO_3$ are available for storage. Mahzoul et al. [10,15] proposed that multiple barium sites are differentiated by their proximity to platinum. Tuttlies et al. proposed that diffusion limits the uptake rate as the nitrate is formed [11]. They pointed out that the large difference in molar volume of the nitrate and carbonate (81.56 and 45.92 cm^3/mol, respectively) suggests that NO/NO_2 must diffuse through a nitrate layer to an underlying barium carbonate layer. A recent study by Stone et al. [8] of a model BaO/Pt(111) catalyst confirms a large increase in particle size during the formation of barium nitrate.

In order to better understand the storage kinetics, we report in Fig. 2 storage data for a range of catalyst temperatures and storage (exposure) times. Shown is NO storage (in moles NO per gram of catalyst) over a range of temperatures for the pre-oxidized catalyst. (We also ran similar experiments with pre-carbonated catalyst and found very similar results for temperatures above 200 °C, although only the results from the pre-oxidized catalysts are shown here.) Beyond 10 min of exposure the storage exhibits two maxima, one above 200 °C and the other at ambient temperature (ca. 25 °C). Each maximum becomes more prominent at longer exposures. The higher temperature maximum occurs at 300 °C for the 20 min exposure, but moves to lower temperatures at longer storage times. After about 5 h of storage time, this maximum occurs at about

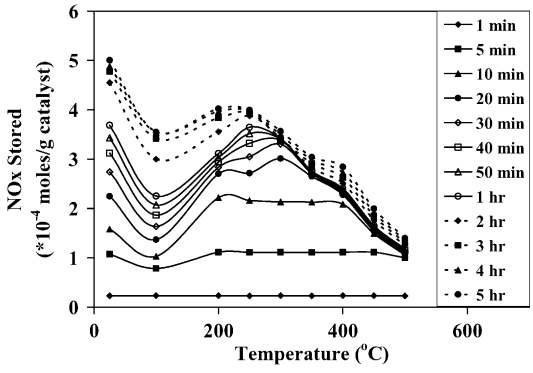

Fig. 2. NO_x stored on $Pt/BaO/Al_2O_3$ catalyst vs. temperature at times ranging from 1 min to 5 h, the feed is 500 ppm NO and 5% O_2 and the catalyst was pre-oxidized at 550 °C for 1 h.

200 °C and total storage decreases monotonically for higher temperatures. The second maximum occurs at ambient temperature conditions, with the NO_x uptake increasing with exposure time.

These detailed data help to elucidate apparent inconsistencies in the literature. The existence of the higher temperature storage maximum is in agreement with previous studies. For example, others have reported that the maximum NO_x capacity is at or near 350 °C [15,22,24]. As Fig. 2 indicates, however, the temperature giving the maximum NO_x uptake is a function of the storage time. This suggests that any comparison of storage data must include the initial state of the catalyst and the storage time.

The storage data also reveal the existence of transport, kinetic, thermodynamic, and dual site uptake effects. At very short exposure times (<5 min), the temperature has a negligible effect on NO_x storage. This could be due to either a NO_x feed limitation to the bed or a mass transfer limitation of the NO_x to the catalyst surface [5]. Our analysis indicates that the former is the more probable limitation. The stronger effect of temperature at longer exposure times reveals the onset of both kinetic and equilibrium factors. To the left of the high temperature maximum the NO_x storage is kinetically limited while to the right of the maximum the reversible decomposition of barium nitrate occurs. Several theories of the kinetic limitation have been proposed in the literature. It is attributed in part to the oxidation of NO to NO_2, since NO_2 is considered to be a key precursor for nitrate formation on barium [16,17]. We have found experimentally, as have others, that NO to NO_2 conversion reaches a maximum near 300 °C [17,26]. (We report data later in the paper.) At temperatures below the maximum, NO_2 production is kinetically limited, which in turn limits the rate of direct nitration of barium sites. A similar mechanism was proposed by Olsson et al. [16], who suggested that the spillover of adsorbed NO_2 from Pt crystallites to adjacent barium oxide sites is an essential, activated step in the storage process with an estimated activation energy of 66 kJ/mol. At high temperatures the barium nitrate formation is clearly equilibrium limited, as the total storage becomes nearly independent of the exposure time. Others have shown that barium nitrate will start to decompose at temperatures as low as 200 °C [28]. If one assumes that NO_2 is needed for storage to occur, then the equilibrium limitation in NO oxidation encountered at temperatures exceeding 300 °C may also play a role. (We investigate this issue in more detail below.) Finally, the second maximum at ambient temperature is likely attributed to either NO adsorption on the alumina support, barium *nitrite* formation, or NO adsorption on platinum. In situ FTIR studies have shown that NO adsorbs on the alumina support at lower temperatures in the presence of O_2 [14]. Also, TPD experiments of NO_x storage at low temperatures (<200 °C) shows two desorption peaks [10,15]. Mahzoul et al. [15] interpret the low temperature desorption peak as nitrate formation from adsorbed nitrites (with NO release).

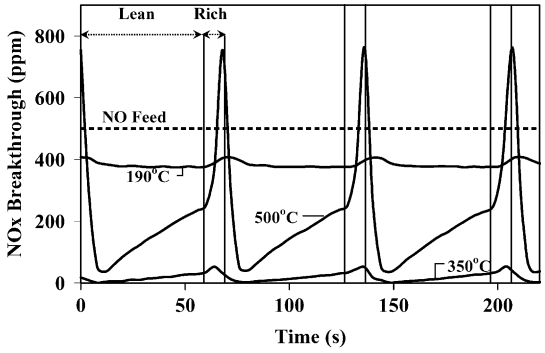

Fig. 3. NO_x breakthrough vs. time for three successive lean/rich cycles on $Pt/BaO/Al_2O_3$ catalyst, the breakthrough at three different feed temperatures (190, 350, and 500 °C) is shown. The lean and rich feed compositions are shown in Table 1.

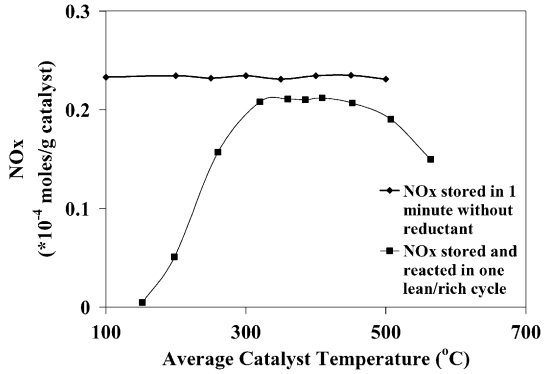

Fig. 4. NO_x stored and/or reacted per gram of $Pt/BaO/Al_2O_3$ catalyst vs. average catalyst temperature for 60 s of non-reactive storage (◆) and one 70 s lean/rich cycle (■). The feed concentrations are shown in Table 1.

Li et al. [10] explain the low temperature adsorption as NO molecular adsorption on platinum. In our case, however, NO adsorption on platinum is not significant enough to account for the large amount of NO_x adsorption at low temperature. More plausible is the adsorption of NO on the support as well as formation of nitrites on the barium component.

In order to relate the storage process to the performance of the catalyst for NO_x reduction, we show in Fig. 3 the NO_x breakthrough obtained during lean/rich cycling for three different feed temperatures (500, 350 and 190 °C). In this set of experiments the lean period lasted for 60 s whereas the rich pulse lasted for 10 s. For reference, time-averaged conversions at the three temperatures were 60, 97, and 23%, respectively (see [3] for details). It is observed at high temperature (500 °C) that a large fraction of NO_x breaks through during the lean storage portion of the cycle. In addition, a significant breakthrough of NO_x occurs during the rich pulse. The large peak indicates that nitrate decomposition and release of NO_x occurs more rapidly than NO_x can be reduced, and in fact the NO_x release during the rich pulse exceeds for a short time the NO_x inlet concentration. The NO_x breakthrough at 350 °C shows a similar trend to that of the one at 500 °C, but the release is much less pronounced, resulting in a higher conversion. The breakthrough at 190 °C exhibits a different trend, a nearly constant level of unconverted NO_x, indicating the equivalent of steady-state lean NO_x conversion at this temperature. These storage features under cycling conditions are not entirely consistent with the storage results obtained on the pre-oxidized catalyst under non-reaction conditions (Fig. 2). Recall in those experiments that the initial NO_x storage is insensitive to temperature, while the storage with cycling indicates a strong temperature dependence. For example, under cycling conditions we see a significant reduction in storage (and conversion) if the temperature is increased from 350 to 500 °C. We attribute these differences to the effect of the reaction on the storage process. More specifically, during reaction both H_2O and CO_2 are present in the gas (due to propylene combustion) which has an adverse effect on the NO_x storage capacity, especially at higher temperatures [18,19]. In addition, the exothermic propylene combustion temporarily increases the catalyst temperature leading to the reversible decomposition of the nitrate.

It is instructive to expand on the connection between short time storage and NO_x conversion. Fig. 4 compares the NO_x storage capacity obtained during a 60 s exposure time on a pre-oxidized catalyst to an estimate of the number of moles of NO (per gram catalyst) reduced during storage and reduction over the same range of temperature. During the storage and reduction experiments large exotherms occur due to propylene combustion, so for comparison purposes, the time-averaged catalyst temperature during the reaction is used here. Note also that the amount of NO converted occurs during one full 70 s lean/rich cycle. There are two notable findings. First, the NO_x stored exceeds the NO_x reacted over the indicated temperature range. This difference is attributed to the CO_2 produced during the reaction which, as mentioned above, causes less NO_x to be stored (and therefore to be reduced). In addition, the catalyst is not completely effective in reducing all of the NO_x stored, as observed in Fig. 3. Second, the utilization of barium during this short time storage is estimated to be only 5%, assuming a stoichiometry of two nitrogen atoms per barium atom. In spite of the small fraction of barium utilized for storage, the catalyst converts over 90% of the NO_x fed between 200 and 400 °C. The results suggest that the 10 s pulse containing 2% propylene is sufficient to regenerate the barium that is utilized for the next storage and reduction cycle. Thus, while the catalyst has ample capacity for additional storage (viz. Fig. 2), it is kinetically inaccessible for the storage and reduction process.

In order to further explore barium utilization during the storage process, the long-time NO_x storage was measured using thermogravimetric analysis (TGA). Fig. 5 shows the TGA-measured uptake of NO on the catalyst for a feed consisting only of NO and O_2 at 350 °C. By comparison, gas phase composition measurement with the FTIR during the microreactor experiments indicated that after approximately 5 h, storage reached a constant value (within the instrument measurement error). For example, in the experiment

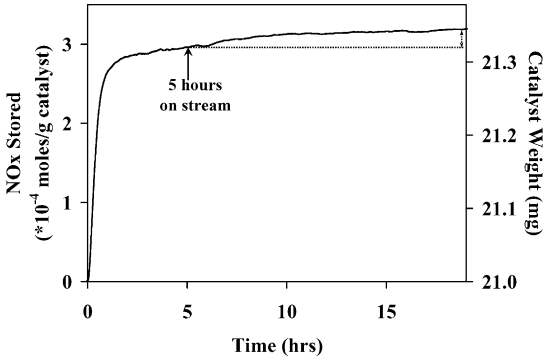

Fig. 5. NO_x stored on $Pt/BaO/Al_2O_3$ catalyst vs. time as determined by weight gain in the TGA for a feed of 500 ppm NO and 5% O_2, and a catalyst temperature of 350 °C.

described in Fig. 1, once the outlet concentration of NO_x reaches a value within 1% of the 500 ppm feed concentration (495 ppm), we were unable to determine if uptake was still occurring. However, for the same feed conditions, the TGA had not yet lined out. Two distinct regimes in the storage are apparent; an initial steep rise in weight followed by a much slower rise. Even after 1200 min (20 h) on stream a steady-state weight was not reached. This suggests that a very slow process is limiting the NO_x uptake. In order to convert weight gain into moles of NO_x we assume that all the barium is initially in the form of barium oxide and that nitrate is the product. We then use the following equations to calculate the net weight gain caused by the adsorption of nitrate:

$$\mathrm{NO}_x\ \text{stored}\left(\frac{\text{mole NO}_x}{\text{g cat}}\right) = \frac{\Delta m\,(\mathrm{g})}{\Delta \mathrm{MW}\,(\mathrm{g/mol})} = \frac{m_{(\mathrm{NO}+\mathrm{O}_2)} - m_{(\mathrm{O}_2)}}{\{\mathrm{MW}_{[\mathrm{Ba(NO_3)_2}]} - \mathrm{MW}_{[\mathrm{BaO}]}\}/2} \quad (1)$$

where m is the weight of the catalyst (under either NO/O_2 or O_2 flow) and MW is the molecular weight of the barium species (either oxide or nitrate). Here we have assumed that the average molecular weight of the stored NO_x species is the difference between the molecular weight of the fully nitrated species and BaO, i.e., $NO_{2.5}$.

Fig. 6a compares long-time storage data obtained in the TGA to that obtained in the microreactor. The experimental conditions in the TGA are similar to those in the microreactor. The catalyst was pretreated in O_2 for 1 h at 550 °C, followed by exposure to a gas containing 500 ppm NO and 5% O_2 for 5 h. A comparison of the TGA and microreactor data shows consistent results. The long-time storage decreases with increasing temperature. Assuming the same 2 N/Ba stoichiometry we find that the maximum barium utilization does not exceed 28% for both the microreactor and TGA studies (Fig. 6b). This underscores the fact that only a fraction of the total barium is available for storage, even after several hours of exposure. These observations are consistent with literature reports. Li et al. [10] differentiated between *bulk* barium and *surface*

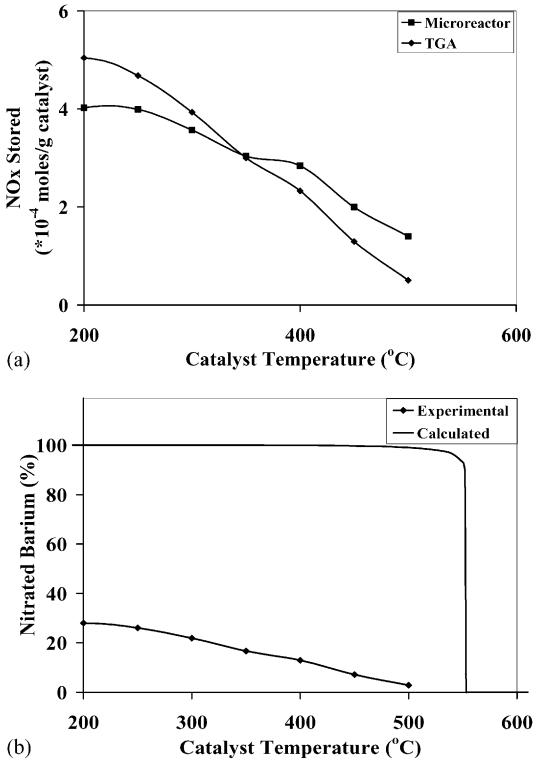

Fig. 6. (a) NO_x stored per gram of $Pt/BaO/Al_2O_3$ catalyst vs. catalyst temperature for 5 h in a flow of 500 ppm NO and 5% O_2 in the microreactor (■) and TGA (◆), (b) the percent of barium oxide converted to barium nitrate vs. catalyst temperature found experimentally after 5 h (◆) and calculated for thermodynamic equilibrium in a closed system (—).

barium, with the surface barium being that which is available for storage. Laurent et al. [29] found that very little barium was involved in the storage (possibly as little as 1%); they state that only grains of BaO which are in close contact with a platinum site can react with NO_2. Hodjati et al. [28] found that bulk barium oxide exhibits much less NO_x storage capacity than that of barium aluminates (barium oxide in an aluminate structure) because bulk barium oxide will form carbonates which are stable to temperatures over 800 °C. Rodrigues et al. [17] found that barium has two forms as well, either large barium carbonate crystals or highly dispersed barium species on the alumina support. They reported that very little NO_x was stored on the bulk barium carbonate species. Prinetto et al. [14] used XRD to show that 30% of the barium is present as crystalline $BaCO_3$ and the other fraction of the barium is amorphous or highly dispersed barium since it could not be detected by XRD. Finally, as stated earlier, Tuttlies et al. [11] proposed that diffusion of NO to underlying barium oxide limits the overall nitration rate.

Fig. 7 reports the steady-state conversion of NO to NO_2 on the same $Pt/BaO/Al_2O_3$ catalyst and for the same conditions as the storage experiments reported in Fig. 6. For comparison, the NO oxidation conversion on Pt/Al_2O_3 is provided. The Pt/Al_2O_3 catalyst exhibits a maximum conversion at about 300 °C, and the $Pt/BaO/Al_2O_3$ catalyst

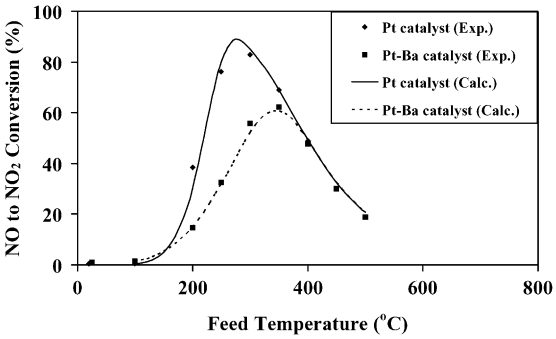

Fig. 7. Comparison of the steady-state conversion of NO to NO_2 on Pt/Al_2O_3 (◆) and Pt/BaO/Al_2O_3 (■) catalysts corresponding to the conditions reported in Fig. 6 (gas feed of 500 ppm NO and 5% O_2, flowing at 200 cm^3/min), and model predictions of NO oxidation for both the Pt/Al_2O_3 (—) and Pt/BaO/Al_2O_3 (- - -) catalysts.

exhibits a maximum conversion at about 350 °C. The maximum reflects the transition between kinetic limitations (lower temperature) and equilibrium limitations (higher temperatures). The results are also consistent with previous results that the Ba-modified catalyst exhibits a reduced NO oxidation activity compared to a Pt catalyst [16].

In order to examine the long-term storage in more detail, we consider a simple model of the adsorptive reactor to simulate the NO_x storage process. We assume that storage occurs via the disproportionation of NO_2, which is produced by the oxidation of NO, i.e.:

$$1: \quad NO + 0.5O_2 \rightleftarrows NO_2,$$

$$\Delta H_1^\circ = -57.1\,\text{kJ/mol}, \ \Delta G_1^\circ = -35.2\,\text{kJ/mol}$$

$$2: \quad 3NO_2 + BaO \rightleftarrows Ba(NO_3)_2 + NO,$$

$$\Delta H_2^\circ = -452\,\text{kJ/mol}, \ \Delta G_2^\circ = -341\,\text{kJ/mol}$$

As discussed earlier, nitrite ($Ba(NO_2)_2$) formation has been observed during exposure of BaO to NO. Moreover, others have reported evidence for a nitrite to nitrate conversion mechanism [5,12,22,23]. However, our intent is to interpret these data with this simple two-step mechanism. Material balances for the reacting species are given by

$$\left(\frac{u_G p_T}{RT\rho_c}\right)\frac{dy_i}{dz} = \sum_j \nu_{ij} r_j \tag{2}$$

where r_j is the net rate of reaction j (mass of catalyst basis), ν_{ij} the stoichiometric coefficient (negative for reactants), ρ_c the catalyst bed density, p_T the total pressure, u_G the superficial linear velocity, y_i the mole fraction of component i, and z the axial distance along the reactor. NO oxidation is assumed to proceed by the following sequence of steps:

I. $O_2 + 2X \leftrightarrow 2O\text{–}X$
II. $NO + X \leftrightarrow NO\text{–}X$
III. $NO\text{–}X + O\text{–}X \leftrightarrow NO_2\text{–}X + X$
IV. $NO_2\text{–}X \leftrightarrow NO_2 + X$
V. $NO + O\text{–}X \leftrightarrow NO_2 + X$

Steps I and II are adsorption of the two reactants, while steps III/IV and V correspond to two possible reaction steps. Step III assumes a surface or Langmuir–Hinshelwood (LH) reaction between adsorbed NO and O, forming adsorbed NO_2 which desorbs according to step IV. Step V corresponds to an Eley–Rideal (ER) reaction between gas phase NO and adsorbed atomic oxygen. If we assume that the overall rate is limited by the LH or ER reaction, we can derive the following rate expressions for the LH mechanism (steps I–IV) and ER mechanism (steps I and V):

$$\begin{aligned}
\text{LH}: \quad r_1 &= k_{LH}(T)p_{NO} \\
&\quad \times \left(\frac{K_{NO}\sqrt{K_{O_2}p_{O_2}}}{(1+\sqrt{K_{O_2}p_{O_2}}+K_{NO}p_{NO}+K_{NO_2}p_{NO_2})^2}\right) \\
&\quad \times \left[1-\left(\frac{1}{K_{e1}(T)}\right)\left(\frac{p_{NO_2}}{p_{NO}p_{O_2}^{0.5}}\right)\right], \\
\text{ER}: \quad r_1 &= k_{ER}(T)p_{NO}\left(\frac{\sqrt{K_{O_2}p_{O_2}}}{1+\sqrt{K_{O_2}p_{O_2}}}\right) \\
&\quad \times \left[1-\left(\frac{1}{K_{e1}(T)}\right)\left(\frac{p_{NO_2}}{p_{NO}p_{O_2}^{0.5}}\right)\right]
\end{aligned} \tag{3}$$

where K_{O_2}, K_{NO}, and K_{NO_2} are oxygen and NO adsorption equilibrium constants. The overall reaction equilibrium constant, $K_{e1}(T)$ is given by the following for the LH and ER mechanisms:

$$\begin{aligned}
K_{e1}(T) &= \left(\frac{p_{NO_2}}{p_{NO}p_{O_2}^{0.5}}\right)_{eq} \\
&= \exp\left(\frac{-\Delta G_1^\circ}{298.2R}\right)\exp\left\{\frac{\Delta H_1^\circ}{298.2R}\left(1-\frac{298.2}{T}\right)\right\} \\
&= \frac{k_{-LH}(T)K_{NO_2}(T)}{k_{LH}(T)K_{NO}(T)K_{O_2}^{0.5}(T)} \quad \text{(LH)} \\
&= \frac{k_{-ER}(T)}{k_{ER}(T)K_{O_2}^{0.5}(T)} \quad \text{(ER)}
\end{aligned} \tag{4}$$

In the limit of a large stoichiometric excess of gas phase oxygen, atomic oxygen is the dominant surface species, such that $(K_{O_2}P_{O_2})^{0.5} \gg 1$. The LH and ER rate expressions then simplify to:

$$\begin{aligned}
\text{LH}: \quad r_{NO_2} &= k'_{LH}(T)p_{NO}\left[1-\left(\frac{1}{K_{e1}(T)}\right)\left(\frac{p_{NO_2}}{p_{NO}p_{O_2}^{0.5}}\right)\right], \\
k'_{LH}(T) &= \frac{k_{LH}(T)K_{NO}(T)}{\sqrt{K_{O_2}(T)p_{O_2}}}; \\
\text{ER}: \quad r_{NO_2} &= k'_{ER}(T)p_{NO}\left[1-\left(\frac{1}{K_{e1}(T)}\right)\left(\frac{p_{NO_2}}{p_{NO}p_{O_2}^{0.5}}\right)\right], \\
k'_{ER}(T) &= k_{ER}(T)
\end{aligned} \tag{5}$$

Thus, both mechanisms predict a first-order dependence on NO with a pseudo first-order rate constant provided in (5).

The steady-state NO_x storage is determined as follows. As stated, the model assumes that the NO_x storage follows the disproportionation mechanism. Under steady-state conditions, the axial concentration profiles of NO, O_2, and NO_2 are established by the NO oxidation reaction. Moreover, the net formation rate of barium nitrate is zero. Thus, the gas phase species profiles determine the local composition of the barium component. Specifically, the solid phase composition is determined by computing the ratio of the apparent equilibrium constant, K_{app}, and the actual equilibrium constant, $K_{e2}(T)$, which is a function only of catalyst temperature:

$$\frac{K_{app}(T)}{K_{e2}(T)} = \frac{p_{NO}/p_{NO_2}^3}{(p_{NO}/p_{NO_2}^3)_{eq}} = \frac{p_{NO}/p_{NO_2}^3}{\exp(-\Delta G_2^\circ/298.2R) \times \exp(\Delta H_2^\circ/298.2R(1-(298.2/T)))} \quad (6)$$

If this ratio exceeds unity, then the equilibrium drives the barium to the oxide state; if the ratio is less than unity, then the barium is in the form of the nitrate. When the ratio is equal to unity this pinpoints the location of a discontinuous change in the barium composition along the length of the reactor.

We used the simple first-order catalytic reactor model to simulate selected experiments. This was done by fitting the NO oxidation conversion data (results in Fig. 7) and then determining the corresponding NO_x storage (results in Fig. 6b). Fig. 7 provides the model predictions of conversion over a range of temperature for both the Pt and Pt/BaO catalysts, while Fig. 6b reports the estimated NO_x storage over the same range for the Pt/BaO catalyst. Table 2 reports the estimated first-order rate parameters, i.e. pre-exponential and activation energy, along with the 95% confidence intervals. The reactor model predictions indicate that the NO oxidation is captured well by the pseudo first-order, reversible kinetics (Fig. 7). At low temperatures NO oxidation is limited by the oxidation rate while at high temperatures it is constrained by equilibrium. The model predicts the existence of two regimes of barium (Fig. 6b). For temperatures below ca. 500 °C the barium exists primarily as the nitrate (except for a very short section at the reactor entrance) while for temperatures exceeding 550 °C barium oxide is the dominant species. For a given feed condition the model predicts the existence of a discontinuity in barium composition along the length of the bed (corresponding to the ratio in Eq. (6) equaling unity). Clearly, the model over-predicts the measured utilization of barium for the entire temperature range of interest. The very large Gibbs free energy change of the disproportionation reaction overwhelms any influence of kinetic limitations of the NO oxidation reaction. The prediction that barium utilization approaches completion for temperatures below 500 °C indicates that there are no thermodynamic limitations. Complete utilization is not encountered experimentally, which suggests that all of the barium is not accessible for nitration, at least within the time scale of hours.

The experimental results show marked differences in the short-term and long-term storage behavior. The short-term storage is a sensitive function of storage time and is nearly independent of temperature, while the long-time storage has much slower kinetics and is a non-monotonic function of temperature. We carried out NO_x storage and reduction in the TGA with the goal of elucidating the effect of the storage dynamics on catalyst performance. A mixture of NO and O_2 was continuously fed to the TGA with intermittent, but regular pulses of reductant (propylene). (The feed concentrations are shown in Table 1.) The intent was, with the in situ mass measurement capability of the TGA, to determine the extent of NO_x uptake during a cycle and the effect of temperature over a much longer operating period.

Fig. 8 shows the dependence of the catalyst mass on time with cycles spanning 7 min in duration (6 min lean; 1 min rich). The catalyst temperature was maintained at a specified level for about 1 h. The data reveal that the weight increased during the lean period and decreased during the rich period, in accordance with NO_x uptake (storage) and removal (release and reduction). Fig. 8b shows a closer view of three cycles at a catalyst temperature of 350 °C. The mass increased slowly during the storage period, which was followed by a sharp increase and then decrease during the propylene pulse. The sharp increase is presumably due to propylene uptake while the decrease is due to propylene and stored NO_x consumption.

An analysis was carried out to determine if the sharp weight increase in weight during the first 15 s of the propylene pulse could be as attributed to propylene adsorption. In the analysis we assumed that the propylene molecularly adsorbs on each exposed platinum site, and used the measured Pt loading (0.47%) and dispersion (47%). We estimated a propylene uptake at saturation of 0.010 mg. The measured uptake during the pulsing experiments was approximately 0.013 mg, suggesting that propylene sorption is responsible for the initial weight increase. As observed in

Table 2
Estimated first-order rate parameters used for modeling

Catalyst	Pre-exponential factor, A (mol/s kg catalyst Pa)	Activation energy (kJ/mol)
Pt/Al_2O_3	68.21 ($36.585 < A < 127.1844$)	65.52 ± 6.75
$Pt/BaO/Al_2O_3$	0.0206 ($0.0109 < A < 0.0386$)	36.03 ± 1.226

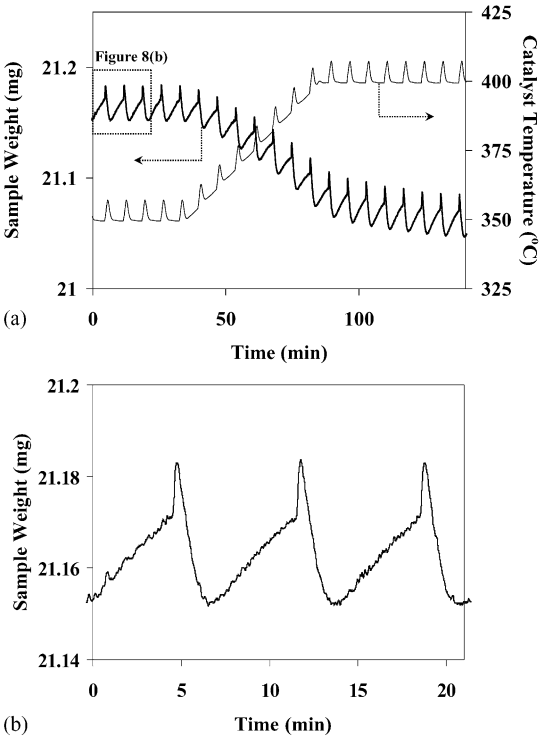

Fig. 8. (a) Pt/BaO/Al_2O_3 catalyst weight and temperature during lean/rich cycling vs. time while transitioning between a furnace temperature of 350 and 400 °C in the TGA, and (b) an enlarged view of the weight changes during three lean/rich cycles at a furnace temperature of 350 °C. The lean time was 6 min and the rich time was 1 min. The lean and rich feed concentrations are listed in Table 1.

Fig. 8a the baseline mass remained approximately constant as long as the feed conditions and system temperature were maintained. Interestingly, when the furnace temperature was increased by ca. 50 °C, a notable drop in the baseline catalyst mass occurred, but the mass and temperature variations during the pulsing remained relatively unaffected. (Note that under non-reactive conditions, there was no measured change in the baseline mass as the temperature was varied over a similar range of values).

These results are consistent with the dynamic process of NO_x storage and reduction superimposed on a longer-term bulk equilibration process. That is, the NO_x storage and reduction process that occurs over the time frame of a single cycle involves a relatively small fraction of the storage component. This is consistent with our earlier finding in which we estimated that only a small fraction of the barium is involved in the NO_x storage and reduction. On the other hand, imposed changes in the feed gas temperature (and hence catalyst temperature) affect the total NO_x uptake in the bulk barium, which is likely determined by equilibrium factors. That is, as the storage data and calculations have revealed, the NO_x storage capacity is a decreasing function of temperature under conditions which favor equilibrium, i.e. high catalyst temperatures and long storage times.

These data are consistent with a surface/bulk process depicted in Fig. 9. The process builds on a picture proposed by Eigenberger and co-workers [11]. The short-time NO_x storage and reduction process, which typically occurs over cycle times not exceeding a few minutes, involves barium that is kinetically accessible, i.e. surface or near-surface barium species. The storage and reduction processes are limited by kinetic and possibly gas phase diffusional processes. On the other hand, changes in feed composition or temperature that occur over a longer period of time will alter the NO_x storage in the less accessible barium, i.e. bulk barium species. The bulk barium will approach an equilibrium composition with kinetics corresponding to a solid-state diffusional process. In summary, consider that a barium carbonate particle contained within the alumina support is exposed to a lean feed. As nitration of the carbonate proceeds, diffusional paths within the individual particles or support may become blocked as a result of carbonate to nitrate particle growth. This will slow the rate of

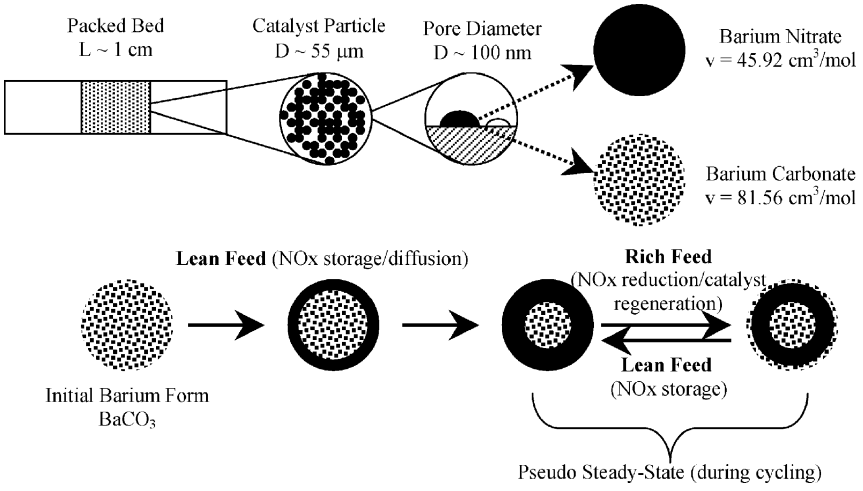

Fig. 9. Schematic of proposed surface/bulk NO_x storage and reduction process.

supply of NO_x to unconverted carbonate. Upon the reintroduction of hydrocarbon, surface nitrate will be regenerated through the reduction chemistry, opening pores for transport. Over many cycles, a continuous supply of NO_x to the catalyst will enable a slow penetration of unreacted NO further into the particle core. Eventually the particle core should approach an equilibrium corresponding to the temperature and NO_x concentration. Clearly, a more detailed picture of this process must emerge through creative experiments and modeling.

4. Conclusions

NO_x storage experiments have been carried out on a model $Pt/BaO/Al_2O_3$ catalyst powder in order to elucidate kinetic and thermodynamic limitations. Storage experiments on a pre-oxidized catalyst reveal that exposure time is an important determinant of storage. The short-term storage is a sensitive function of storage time and is nearly independent of temperature, whereas the long-time storage has much slower kinetics and is a non-monotonic function of temperature. The data indicate that less than 10% of the barium is needed to achieve over 90% NO_x reduction. In situ mass measurements during NO_x storage and reduction corroborate a physical picture in which a small fraction of barium is used while the remainder approaches a bulk composition that is in equilibrium with the bulk gas. A simple model is constructed that predicts NO oxidation conversion and NO_x storage. The results suggest that full barium utilization is thermodynamically feasible even under kinetically limited conditions of incomplete NO oxidation. However, diffusion limitations may prevent complete utilization. At high temperature both NO oxidation and barium nitrate formation are thermodynamically limited, both of which adversely impact the NO_x reduction.

Acknowledgements

The support of the State of Texas Advanced Technology Program (ATP) is gratefully acknowledged. We also acknowledge fruitful technical discussions with Dr. Yuejin Li of Engelhard Corporation and Dr. Gregor Kolios of the University of Stuttgart.

References

[1] N. Takahashi, H. Shinjoh, T. Iijima, T. Suzuki, K. Yamazaki, K. Yokota, H. Suzuki, N. Miyoshi, S.I. Matsumoto, T. Tanizawa, T. Tanaka, S.-S. Tateishi, K. Kasahara, Catal. Today 27 (1996) 63.
[2] T. Miyoshi, S.I. Matsumoto, K. Katoh, T. Tanaka, J. Harada, N. Takahashi, K. Yokota, M. Sugiura, K. Kasahara, SAE J.-Automot. Eng. 950809 (1995) 1361.
[3] R.L. Muncrief, K.S. Kabin, M.P. Harold, AIChE J. 50 (2004) 2526.
[4] J. Jirat, M. Kubicek, M. Marek, Catal. Today 53 (1999) 583.
[5] H.Y. Huang, R.Q. Long, R.T. Yang, Energ. Fuel 15 (2001) 205.
[6] S. Salasc, M. Skoglundh, E. Fridell, Appl. Catal. B: Environ. 36 (2002) 145.
[7] M. Machida, Catalysis 15 (2000) 73.
[8] P. Stone, M. Ishii, M. Bowker, Surf. Sci. 537 (2003) 179.
[9] S. Hodjati, P. Bernhardt, C. Petit, V. Pitchon, A. Kiennemann, Appl. Catal. B: Environ. 19 (1998) 221.
[10] X. Li, M. Meng, P. Lin, Y. Fu, T. Hu, Y. Xie, J. Zhang, Top. Catal. 22 (2003) 111.
[11] U. Tuttlies, V. Schmeisser, G. Eigenberger, Proceedings of the Sixth International Congress on Catal. and Automot. Poll. Control, Brussels, Belgium, October 22–24, 2003.
[12] P.J. Schmitz, R.J. Baird, J. Phys. Chem. B 106 (2002) 4172.
[13] E. Fridell, M. Skoglundh, B. Westerberg, S. Johansson, G. Smedler, J. Catal. 183 (1999) 196.
[14] F. Prinetto, G. Ghiotti, I. Nova, L. Lietti, E. Tronconi, P. Forzatti, J. Phys. Chem. B 105 (2001) 12732.
[15] H. Mahzoul, J.F. Brilhac, P. Gilot, Appl. Catal. B: Environ. 20 (1999) 47.
[16] L. Olsson, H. Persson, E. Fridell, M. Skoglundh, B. Andersson, J. Phys. Chem. B 105 (2001) 6895.
[17] F. Rodrigues, L. Juste, C. Potvin, J.F. Tempere, G. Blanchard, G. Djega-Mariadassou, Catal. Lett. 72 (2001) 59.
[18] N.W. Cant, M.J. Patterson, Catal. Lett. 85 (2003) 153.
[19] W.S. Epling, G.C. Campbell, J.E. Parks, Catal. Lett. 90 (2003) 45.
[20] N.W. Cant, M.J. Patterson, Catal. Today 73 (2002) 271.
[21] E. Fridell, H. Persson, B. Westerberg, L. Olsson, M. Skoglundh, Catal. Lett. 66 (2000) 71.
[22] L. Lietti, P. Forzatti, I. Nova, E. Tronconi, J. Catal. 204 (2001) 175.
[23] F. Prinetto, G. Ghiotti, I. Nova, L. Castoldi, L. Lietti, E. Tronconi, P. Forzatti, Phys. Chem. Chem. Phys. 5 (2003) 4428.
[24] E. Fridell, M. Skoglundh, S. Johansson, B. Westerberg, A. Torncrona, G. Smedler, Stud. Surf. Sci. Catal. 116 (1997) 537.
[25] I. Nova, L. Castoldi, L. Lietti, E. Tronconi, P. Forzatti, Catal. Today 75 (2002) 431.
[26] L. Olsson, B. Westerberg, H. Persson, E. Fridell, M. Skoglundh, B. Andersson, J. Phys. Chem. B 103 (1999) 10433.
[27] L. Olsson, E. Fridell, M. Skoglundh, B. Andersson, Catal. Today 73 (2002) 263.
[28] S. Hodjati, P. Bernhardt, C. Petit, V. Pitchon, A. Kiennemann, Appl. Catal. B: Environ. 19 (1998) 209.
[29] F. Laurent, C.J. Pope, H. Mahzoul, L. Delfosse, P. Gilot, Chem. Eng. Sci. 58 (2003) 1793.